Alternate erosion and deposition in the Yangtze Estuary and its future change

Alternate erosion and deposition in the Yangtze Estuary and its future change

Zhu Boyuan [1], Li Yitian [2], * Yue Yao [2], Yang Yunping [3], Liang Enhang [4], Borthwick Alistair G. L. [5]

1. School of Hydraulic Engineering, Key Laboratory of Water-Sediment Sciences and Water Disaster Prevention of Hunan Province, Changsha University of Science & Technology, Changsha 410114, China
2. School of Water Resources and Hydropower Engineering, State Key Laboratory of Water Resources and Hydropower Engineering Science, Wuhan University, Wuhan 430072, China
3. Key Laboratory of Engineering Sediment, Tianjin Research Institute for Water Transport Engineering, Ministry of Transport, Tianjin 300456, China
4. The Key Laboratory of Water and Sediment Sciences，Ministry of Education; College of Environmental Sciences and Engineering，Peking University，Beijing 100871, China
5. School of Engineering, The University of Edinburgh, The King's Buildings, Edinburgh EH9 3JL, UK

Foundation: Youth Project of National Natural Science Foundation of China, No. 41601275

Author: Zhu Boyuan (1989-), PhD, Lecturer, specialized in estuarine and coastal evolution and causes. E-mail: boyuan@csust.edu.cn

*** Correspondence author:** Yue Yao (1986-), PhD, Lecturer, E-mail: yueyao@whu.edu.cn

Abstract: The morphological changing trend of the Yangtze Estuary, the largest estuary in Asia, has become a focus of research in recent years. Based on a long series of topographic data from 1950 to 2015, this paper studied the erosion-deposition pattern of the entire Yangtze Estuary. Alternating erosion and deposition has occurred during the past 65 years, corresponding to changes between flood and dry periods identified by multi-year average duration days of high-level water flow (defined as discharge ≥ 60,000 m^3/s, namely, $D_{\geq 60,000}$) from the Yangtze River Basin. A quantitative relationship was proposed between the erosional/depositional rate of the Yangtze Estuary and the interpreting variables of yearly water discharge, $D_{\geqslant 60,000}$ and yearly river sediment load, with contributing proportions of 1%, 59% and 40%, respectively. The mechanism behind the alternate erosion and deposition pattern was analyzed by examining the residual water surface slope and the corresponding sediment transport capacity in flood and dry periods. In flood periods, a larger discharge results in a steeper-sloped residual water level, which permits a greater sediment transport capacity. Therefore, more bed material can be washed to the sea, leading to erosion of the estuary. In contrast, a flatter slope in residual water level occurs in dry periods, and deposition dominates the estuarine area due to the decreased sediment transport capacity and the increased backwater effect of the flood-tide. Coastal dynamics and estuarine engineering projects impacted on local morphological changes, but slightly affected the total erosional/depositional rate of the whole estuarine region. Heavy sedimentation within the Yangtze Estuary after the impoundment of the Three Gorges Dam was attributed to the reduced occurrence frequency of flood years due to water regulation by the dam, and largely (at least 36-52%) sourced from the sea. Deposition could still occur in the Yangtze Estuary in the future, because the multi-year average $D_{\geq 60,000}$ is unlikely to exceed the critical value of 14 days/yr corresponding to the future equilibrium state of the Yangtze Estuary, under the water regulation of large cascade dams in the upper Yangtze. Nevertheless, the mean depositional rate is highly unlikely to surpass the peak value of

the past years, because of the decreasing trend in total sediment load entering the Yangtze Estuary.

Keywords: Yangtze Estuary; erosion and deposition; alternation; total sediment load; evolutional trend

1 Introduction

As the largest estuary in Asia, The Yangtze Estuary is located at the distal end of the Yangtze River (Figure 1a) which ranks third, fourth and fifth respectively in terms of length, sediment load and water discharge among the world's rivers (Yang S L *et al.*, 2015). Covering the most prosperous regions in China (namely, Shanghai Municipality and Jiangsu Province, Figure 1b), the estuarine area of Yangtze provides excellent shipping conditions (Dai *et al.*, 2013) and abundant land resources (Chen *et al.*, 2016), attracting the interest from morphologists worldwide.

Existing studies have widely investigated the impacts of river fluxes, coastal hydrodynamics and human interferences on the subaqueous or subaerial terrain within the Yangtze River Delta, pointing out that different areas have experienced different topographic changes under the influences of various determinant factors in the last few decades. For instance, erosion was found in the area between Datong and Xuliujing (Zheng *et al.*, 2018), between -5 m and -8 m water depths downstream of Xuliujing (Yang *et al.*, 2011), the South Branch (Luan *et al.*, 2016; Zhao *et al.*, 2018), the upper reach of the North Channel (Mei *et al.*, 2018), the adjacent outer area off the North Branch (Luo *et al.*, 2017) and the Yangtze subaqueous delta front (Luo *et al.*, 2017; Yang *et al.*, 2018), mainly due to sediment trapping effect of river dams, construction of embankments, and management of estuarine channels. However, deposition was detected in the submerged delta ranging from 121.78° E to 122.67° E and from 30.82° N to 31.53° N (Dai *et al.*, 2014a), covering the mouth bar area (the North Passage, the South Passage and the lower reach of the North Channel included) (Dai *et al.*, 2013, 2015; Luan *et al.*, 2016; Li *et al.*, 2018; Mei *et al.*, 2018; Zhao *et al.*, 2018), the North Branch (Dai *et al.*, 2016; Luo *et al.*, 2017) and the tidal flats (Du *et al.*, 2016), primarily due to marine hydrodynamics (e.g., flood tides, storm surges, waves, hyperpycnal plumes, alongshore currents) and human

activities (e.g., truncation of peak floods by dams, the Deepwater Channel Project and land reclamation), which offset the effects of reduced river sediment supply by carrying local or marine sediment. In addition, equilibrium was identified in several runnels within the South Branch (Wang *et al.*, 2008, 2013) and at the Jiuduan Shoal (Jiang *et al.*, 2012), dominated by the influences of reduced sediment load from rivers, landward propagation of tidal wave and human interferences. Accordingly, evolutionary trends have been predicted to be driven by erosion (Yang *et al.*, 2011; Luan *et al.*, 2017; Luo *et al.*, 2017; Yang *et al.*, 2018), deposition (Dai *et al.*, 2016; Li *et al.*, 2016; Li *et al.*, 2018; Wei *et al.*, 2016, 2017) or equilibrium (Guo *et al.*, 2015; Zhu *et al.*, 2016; Chen Y *et al.*, 2018; Zhao *et al.*, 2018) in different sub-areas in response to the changes of relevant factors.

Previous research has provided insight into the morphological changes in the Yangtze Estuary from the perspective that the estuary may suffer from erosion, deposition or equilibrium, rather than unidirectional erosion, even though the river sediment discharge has largely decreased. Moreover, water discharge and sediment load from the river, and tidal current have been identified as primary factors in the morphological evolution of the Yangtze Estuary. Meanwhile, estuarine engineering projects have extended impacts beyond their given sites. Although the factors related to river sediment load, tidal current, and estuarine engineering projects have been studied by many researchers (Chen *et al.*, 1982; Wang *et al.*, 2008, 2013; Li *et al.*, 2011; Yang *et al.*, 2011; Dai *et al.*, 2014a, 2016; Luan *et al.*, 2016, 2017; Luo *et al.*, 2017; Chen Y *et al.*, 2018; Mei *et al.*, 2018; Yang *et al.*, 2018; Zhao *et al.*, 2018), river water discharge has not been adequately explored, especially at large scale over long periods (Wang *et al.*, 2013; Guo *et al.*, 2015; Luan *et al.*, 2016; Wei *et al.*, 2016, 2017; Zhu *et al.*, 2017; Mei *et al.*, 2018; Zhang *et al.*, 2018). In particular, how the hydrological behavior of periodic alternations between flood and dry periods of the Yangtze Basin will affect large-scale morphological changes of the estuary needs to be answered, in order to forecast the long-term evolution of the Yangtze Estuary in the future. In addition, sediment flux coming from the sea may also affect the evolutional trend of morphology (Dai *et al.*, 2014a, 2016; Chen Y *et al.*, 2018; Mei *et al.*, 2018). However,

existing predictions have mainly based on the long-term variation of the river sediment discharge (Yang *et al.*, 2011; Luan *et al.*, 2017; Luo *et al.*, 2017; Yang *et al.*, 2018). Thus, the long-term changing trends of both marine and riverine supplies of sediment need also to be dissected to get an overall perception of the future evolution of the Yangtze Estuary.

In order to provide a better understanding of the connection between the river water discharge and the large-scale, long-period evolution of Yangtze Estuary, the present study investigated variations in total erosion and deposition during different hydrological periods based on terrain data from the submerged delta of the entire estuary, collected from 1950 to 2015. A quantitative relationship between erosional/depositional rate and river fluxes has been developed, and the mechanism behind morphological evolution patterns in relation with hydrological cycles further investigated. In addition, the long-term changing trends of both riverine and marine sediment sources have also been analyzed. Thus, future evolution in morphology of the Yangtze Estuary can be fairly predicted. This study is also of significance to other estuaries experiencing great changes in riverine hydrological processes and sediment supplies from either river basins or sea area.

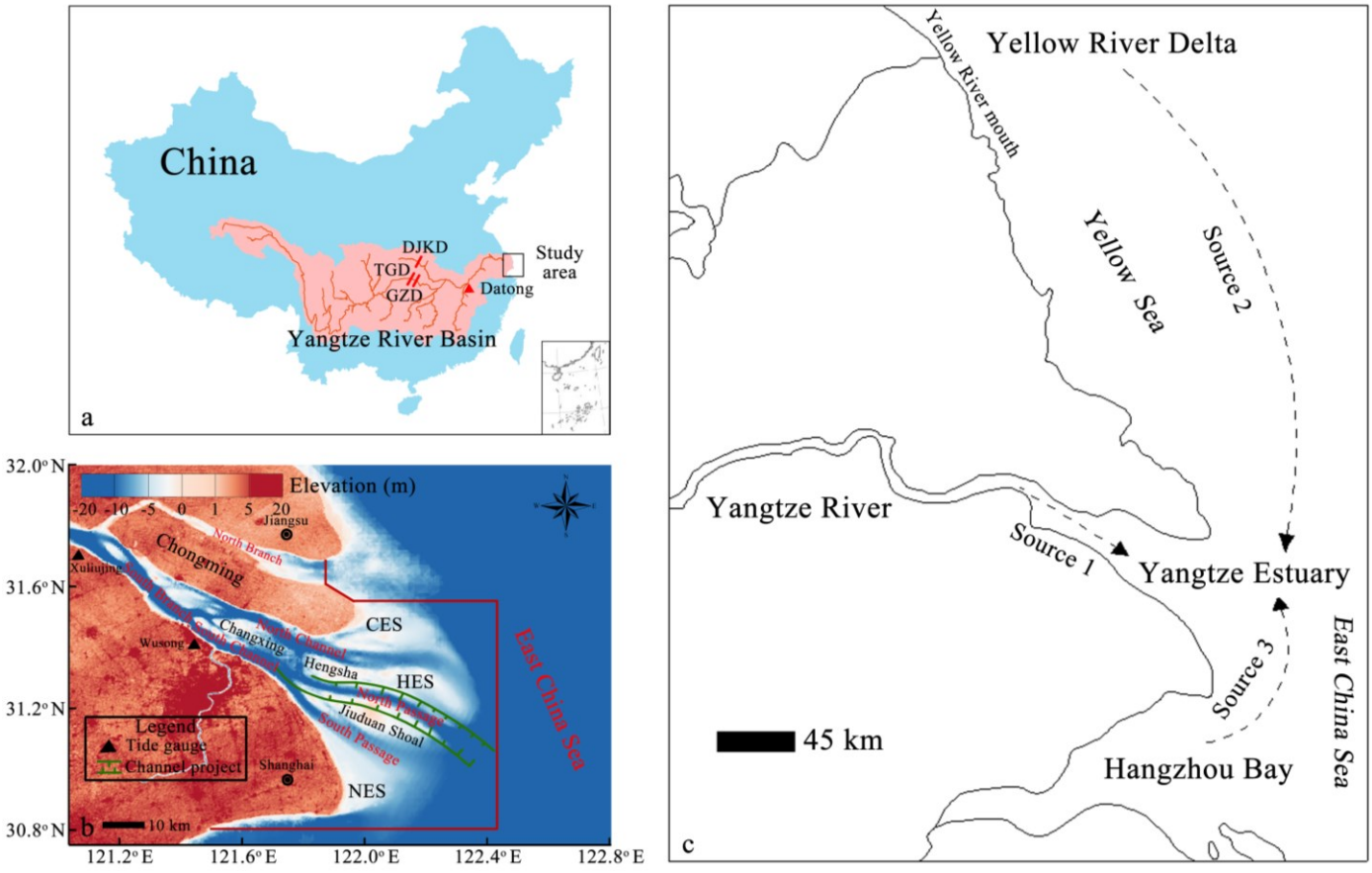

Figure 1 Important locations and geographical features of the Yangtze Estuary. (a) Locations of the Datong station, the Three Gorges Dam (TGD), the Gezhou Dam (GZD) and the Danjiangkou Dam (DJKD) within the Yangtze River Basin of China, and the Yangtze Estuary (the study area). (b) Plan view of the Yangtze Estuary; CES, HES and NES represent Chongming East Shoal, Hengsha East Shoal, and Nanhui East Shoal, respectively; region enclosed by the red line almost covers the entire Yangtze Estuary downstream of Xuliujing, which is identical to that in Chen Y *et al.* (2018) providing the major dataset of total erosional/depositional rate in this study. (c) Major sediment sources of the Yangtze Estuary.

2 Geographical setting

The Yangtze Estuary downstream of Xuliujing stretches 180 km from west to east and 6-90 km from north to south at the tail end of the Yangtze River (Figure 1a), where the channels present a three-fold bifurcating structure (Figure 1b): at Chongming Island, the river forms the first bifurcation fold where it divides into the North Branch and the South Branch; the South Branch then bifurcates at Changxing and Hengsha Island and branches as the North Channel and the South Channel; the South Channel again splits at the Jiuduan Shoal, forming the North Passage and the South Passage. At the mouth area, there are three large tidal flats named Chongming East Shoal (CES), Hengsha East Shoal (HES), and Nanhui East Shoal (NES) from north to south (Figure 1b). The Yangtze Estuary is meso-tidal with a mean tide range of 2-3 m and a flow velocity of about 1 m/s (Li *et al.,* 2011; Zhang *et al.,* 2016), receiving water and sediment from both the river and the sea. The annual average river water discharge is about 28,300 m^3/s at Datong station (thereafter Datong) (CWRC, 2015), the last hydrological station (～500 km upstream from the estuary, see Figure 1a) which retains long-term water and sediment discharge records for the river basin and is usually regarded as the representative station for the river fluxes into the estuary (Yang *et al.*, 2011; Dai *et al.*, 2014a; Luan *et al.*, 2016, 2017; Zhu *et al.*, 2017; Fu, 2018; Mei *et al.*, 2018; Yang *et al.*, 2018; Zhao *et al.*, 2018). The annual average flood-tide current is approximately nine times larger than the river discharge (Chen and Li, 2002). The annual average river sediment load observed at Datong has decreased drastically from 4.25×10^8 t/yr during 1951-2002 to 1.39×10^8 t/yr during 2003-2015 due to the construction of dams and the

implementation of soil conservation measures within the river basin (CWRC, 2015; Fu, 2018). In addition to sediment from the river basin, sediment from the sea is supplied from three sources: sediment carried by the longshore current from the Yellow River Delta; material brought by littoral flow from the Hangzhou Bay; and earlier storage within the offshore area transported by river water from the watershed (Lin, 1988). For simplicity, the third source of marine sediment is also regarded as from the Yangtze River Basin. Figure 1c shows all possible pathways of sediment supplied to the Yangtze Estuary.

3 Data and Methods

3.1 Data sources

Observed daily water discharge and yearly sediment load time series from 1950 to 2015 at Datong were supplied by the Changjiang Water Resources Commission, China. The multi-year average rate of morphological change of the large submerged delta of the Yangtze Estuary during 1958-2015 is estimated from data in the open literature (Dai *et al.*, 2014a; Chen Y *et al.*, 2018) and navigational charts of the Yangtze Estuary in 1997, 2002 and 2007 (provided by Changjiang Water Resources Commission, China, and the Shanghai Estuarine & Coastal Science Research Center, China). Yearly dredging volume associated with the Deepwater Channel Project was obtained from the Shanghai Estuarine & Coastal Science Research Center (China). Other supporting data on water, typhoon, sediment, and reclamation parameters were also collected from previous researches: (1) residual water level between Xuliujing and the river mouth varying with runoff discharge in 2005 (Cai *et al.*, 2014a); (2) major typhoon events that occurred in the Yangtze estuarine area during 1950-2015 (Dai *et al.*, 2014a; Chen Y *et al.*, 2018; Liu *et al.*, 2019); (3) multi-year mean net sediment fluxes at Xuliujing and the river mouth during 2002-2009 (Yang Y P *et al.*, 2014); (4) monthly suspended sediment concentrations at Datong and Xuliujing during 1958-2009 (Yang Y P *et al.*, 2015); (5) yearly suspended sediment concentrations in the Yellow River Delta and Hangzhou Bay during 1998-2009 (Li, 2012; Zhang *et al.*, 2014); (6) Multi-year average reclamation rate in the Yangtze Estuary during 1960-2015 (Chen L *et al.*, 2018). Table 1 summarizes all the data sources of this study.

Table 1 Data sources of this study.

Type	Name	Period(s)	Source(s)
Hydrodynamics	Daily river water discharge at Datong	1950-2015	Changjiang Water Resources Commission
	Residual water level between Xuliujing and the river mouth varying with runoff discharge	2005	Cai *et al.*, 2014a
	Typhoon in the Yangtze estuarine area	1950-2015	Dai *et al.*, 2014a; Chen Y *et al.*, 2018; Liu *et al.*, 2019
Sediment	Yearly river sediment load at Datong	1951-2015	Changjiang Water Resources Commission
	Multi-year average net sediment fluxes at Xuliujing and the Yangtze river mouth	2002-2009	Yang Y P *et al.,* 2014
	Monthly suspended sediment concentrations at Datong and Xuliujing	1958-2009	Yang Y P *et al.,* 2015
	Yearly suspended sediment concentrations in the Yellow River Delta and the Hangzhou Bay	1998-2009	Li, 2012; Zhang *et al.,* 2014
Terrain	Navigational charts of the Yangtze Estuary	1997, 2002	Changjiang Water Resources Commission
		2007	Shanghai Estuarine & Coastal Science Research Center
	Multi-year average morphological change rates of the Yangtze Estuary	1958-2002, 2002-2009	Dai *et al.,* 2014a
		1958-1983, 1983-1997, 1997-2002, 2002-2009, 2009-2013, 2013-2015	Chen Y *et al.,* 2018
	Yearly dredging volume associated with the Deepwater Channel Project	2000-2015	Shanghai Estuarine & Coastal Science Research Center
	Multi-year average reclamation rate in the Yangtze Estuary	1960-1980, 1980-2000, 2000-2010, 2010-2015	Chen L *et al.*, 2018

3.2 Processing of river water discharge

The number of days in which the discharge exceeded or equaled 60,000 m^3/s (thereafter $D_{\geq 60,000}$) was determined for each of the years from 1950 to 2015, based on the time series of daily water discharge at Datong, to reflect the annual severity of fluvial flood events. Herein, 60,000 m^3/s was adopted as a critical discharge because it is the level of multi-year average peak-flood discharge from 1950 to 2015 at Datong (i.e. 58,300 m^3/s), and also approaches the effective/bankfull discharge (i.e. 60,400 m^3/s; Yun, 2004; Luan *et al.*, 2016) of the Yangtze Estuary, regarded as the dominant discharge required for significant bed-level changes

(Andrews, 1980; Emmett and Wolman, 2001; Yun, 2004; Gomez *et al.,* 2007; Xia *et al.,* 2014; Luan *et al.*, 2016). Moreover, annual mean duration days of different discharge levels were also calculated to depict the variability of river water discharge within the period of interest.

3.3 Processing of navigational charts

In addition to data on the morphological change rate of the Yangtze Estuary directly extracted from published literature, three sets of navigational charts surveyed from between early May/June to the end of July in 1997, 2002 and 2007 were also collected. To process these charts, an automatic transfer from their original projections onto Beijing 54 coordinates was conducted using ArcGIS 10.2, with reference to the theoretical low-tide datum at Wusong (Figure 1b) during the digitization. Bed-elevations and positions of the points in the charts were acquired using dual-frequency echo sounders and GPS positioning, respectively. Measurement errors were ± 0.1 m for bed-elevation, and ± 1m for position; these are generally acceptable values, given that bed-elevation changes over decades can be very huge, making the relative error very small (Luan *et al.*, 2016). The average sampling density is between 3 and 12 points per km^2 (i.e., spacing of between 0.3 and 0.6 km between two adjacent points), which appears sufficiently representative because terrain changes per km of the Yangtze Estuary are usually gradual (Wang *et al.*, 2008). Terrain changes were calculated by means of Kriging interpolation at grid resolution of 160 m × 120 m. It should be noted that the present study explores the overlapping area of the three sets of navigational charts extending from 121.78° E to 122.34° E and from 30.96° N to 31.46° N, to compare temporal changes in morphology.

4 Results and discussion

4.1 Alternate erosion and deposition during flood and dry periods

Figure 2a shows that three erosion-deposition cycles affected the submerged area marked by red line in Figure 1b. Cycle 1 started with erosion around 1954, and followed by heavy deposition during 1958-1983 and erosion-deposition equilibrium during 1983-1997. Cycle 2 consisted of erosion during 1997-2002 and deposition during 2002-2009. Cycle 3 presented as severe erosion during 2009-2013 and heavy deposition

during 2013-2015. The finding that erosion occurred about 1954 is supported by Wu *et al.* (2003), Yun (2004) and He *et al.* (2013) all of whom reported erosion in the Yangtze mouth bar area and the formation of the North Passage, even though no topographic data was available before 1958.

Figure 2b illustrates that the yearly river water discharge from 1950 to 2015 did not exhibit an obvious trend, whereas the yearly river sediment load decreased significantly after 1985. By comparison with the erosion and deposition series in Figure 2a, it appears that each of the erosion and deposition cycles in the marked submerged area commenced in a flood period (i.e., a period with higher value of $D_{\geq 60,000}$. The three flood periods contained typical flood years of 1954, 1998 (1999) and 2010, respectively.) In other words, erosion co-occurred with flood periods, and immediately alternated with deposition in dry periods.

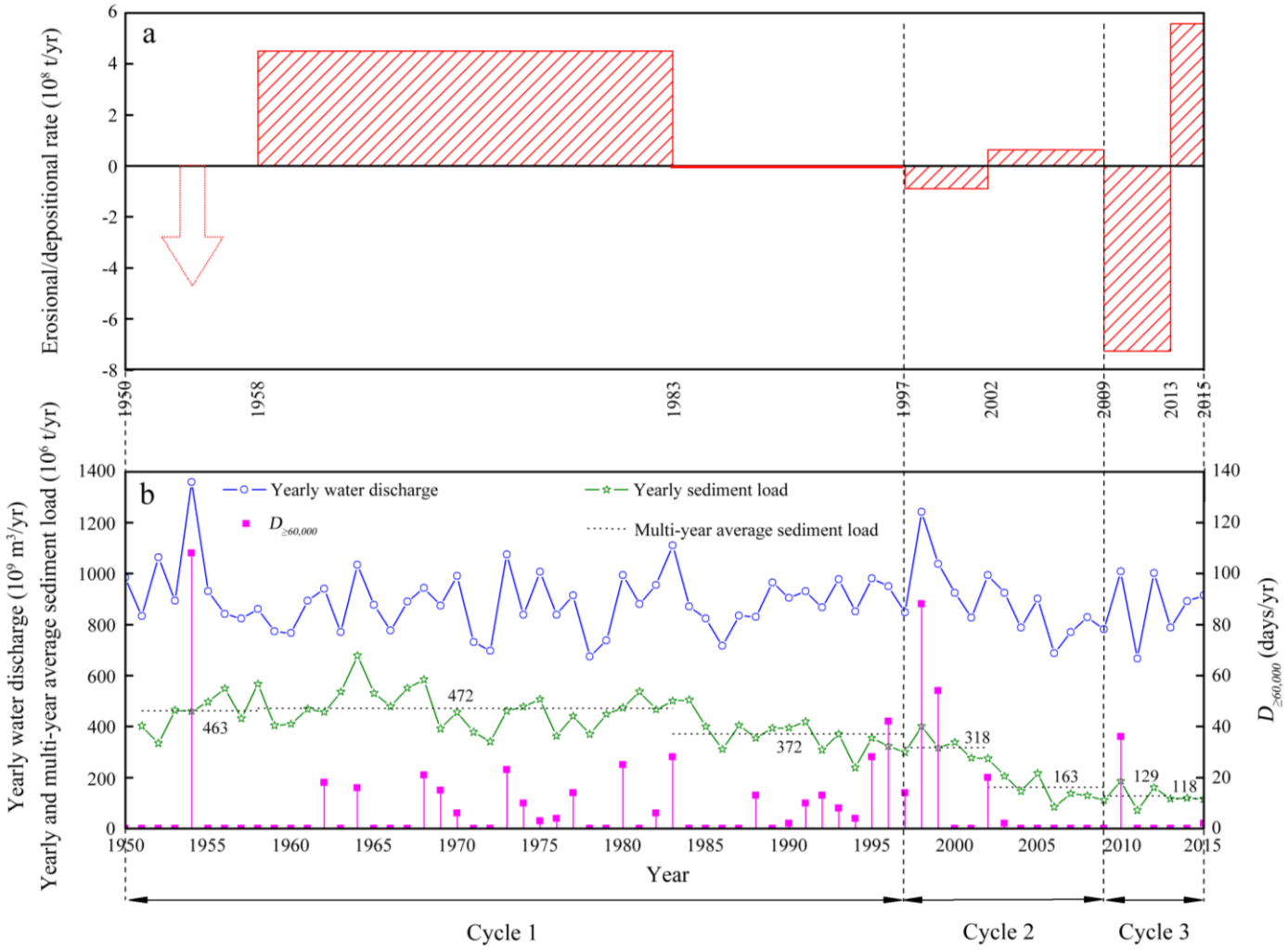

Figure 2 Comparison between morphological and hydrological processes in the Yangtze Estuary. (a) Histogram of erosional/depositional rates (positive values indicating deposition, and negative ones representing erosion) of the marked submerged area (Figure 1b) in the periods of 1950-1958, 1958–1983, 1983–1997, 1997–2002, 2002–2009, 2009–2013 and

2013–2015, respectively; the dashed arrow during 1950-1958 represents an erosional state of the marked submerged area and the red-bold line segment over 1983-1997 stands for an equilibrium state. (b) Yearly river water discharge, $D_{\geq 60,000}$ and yearly and multi-year average river sediment load at Datong from 1950 to 2015.

Although previous studies have observed that episodic cycles of erosion during extreme flood periods and readjustments during following dry periods occurred in component regions within the Yangtze Estuary (Mei *et al.*, 2018) and within other estuarine systems (Cooper, 2002), the present study implies that such cycles can also happen in an entire estuarine area.

4.2 Mechanism behind erosion-deposition alternation

4.2.1 Quantitative relationship between erosional/depositional rate and river fluxes

Table 2 lists linear regression equations linking the erosional/depositional rate of the entire Yangtze Estuary and interpreting variables of the yearly river water discharge, the $D_{\geq 60,000}$ and the yearly river sediment load, derived from the data in Figure 2. The erosional/depositional rate loosely correlates with one single factor (Eqs. (1)～(3)), but tightly correlates with multiple factors (Eqs. (4)～(7)), especially with the combination of yearly river water discharge and $D_{\geq 60,000}$ (Eqs. (6) and (7)). When the yearly river sediment load is added, the correlation is further improved (Eq. (7)). Moreover, the coefficients for yearly river water discharge and yearly river sediment load in Equation (7) are positive, suggesting that heavier deposition will occur as the two variables increase, given that higher annual river water discharge carries higher annual river sediment load. By contrast, the coefficient before $D_{\geq 60,000}$ is negative, leading to more severe erosion when $D_{\geq 60,000}$ increases. Equation (7) exhibits a reasonable relationship between water-sediment conditions and morphological change, and so is adopted in this study.

Table 2 Linear regression fits to the erosional/depositional rate of the entire Yangtze Estuary interpreted by river fluxes [a].

Case	Factor(s) considered	Equation	R^2
(1)	V	$EDR = 0.00002V + 0.277$	0.000
(2)	$D_{\geq 60,000}$	$EDR = -0.123D_{\geq 60,000} + 1.623$	0.077
(3)	S	$EDR = 0.921S - 1.982$	0.087
(4)	V and S	$EDR = -0.002V + 1.184S + 11.345$	0.112

(5)	$D_{\geqslant 60,000}$ and S	$EDR = -0.21D_{\geqslant 60,000} + 1.512S - 1.502$	0.275
(6)	V and $D_{\geqslant 60,000}$	$EDR = 0.021\ V - 1.136\ D_{\geqslant 60,000} - 178.434$	0.714
(7)	V, $D_{\geqslant 60,000}$ and S	$EDR = 0.02V - 1.092D_{\geqslant 60,000} + 0.731S - 164.706$	0.756

[a] V (10^8 m^3/yr), $D_{\geqslant 60,000}$ (days/yr), S (10^8 t/yr) and EDR (10^8 t/yr) represent the multi-year average values of annual river water discharge, duration days of discharge level ≥60,000 m^3/s, annual river sediment load and erosional/depositional rate of the entire Yangtze Estuary, respectively, and R^2 stands for the correlation coefficients of the linear regressions.

According to Equation (7), the annual river water discharge, $D_{\geqslant 60,000}$ and annual river sediment load contribute 1%, 59% and 40% (obtained through dividing the absolute values of the coefficients before the interpreting variables by the sum of the absolute values), respectively, to the erosional/depositional rate, which indicates that $D_{\geqslant 60,000}$ and yearly river sediment load separately play the dominant and secondary roles in morphological alternations of the entire Yangtze Estuary. Erosional/depositional rates of the entire Yangtze Estuary in 1954, 1998 (1999) and 2010 calculated using Equation (7), based on corresponding values of yearly river water discharge, $D_{\geqslant 60,000}$ and yearly river sediment load in Figure 2(b), are -7.44×10^8 t/yr, -9.37×10^8 t/yr (-13.85×10^8 t/yr) and -1.10×10^8 t/yr. This demonstrates that flood events in these years caused significant erosion (Figure 2a). The calculated erosional rate in 2010 is much smaller than that during the 2009-2013 period because the yearly river sediment load in 2011 was very low (Figure 2b), making the erosional rate very large (-30.76×10^8 t/yr, calculated using Eq. (7)) in this year and enhancing the multi-year average erosional rate during 2009-2013. Although $D_{\geqslant 60,000}$ decreases sequentially in 1954, 1998, and 1999 (Figure 2b), the calculated erosional rate increases accordingly, being related to the successive decrease in annual river sediment loads in these three years (Figure 2b). These phenomena indicate the impact of annual river sediment load in the morphological evolution of the entire Yangtze Estuary.

4.2.2 Confrontation between runoff and flood tide

Given that $D_{\geqslant 60,000}$ acts as the dominant factor in controlling the erosion-deposition alternation of the entire Yangtze Estuary, an in-depth analysis of the hydrodynamic changes can reveal the mechanism behind the

water-morphology process. Runoff and tide are two major hydrodynamic drivers in the morphological processes of estuaries. During the flood tide, the two drivers act in opposition with one flowing seaward and the other landward, with the scale of confrontation mainly determined by river water discharge, noting the relative stability of flood-tide current in estuaries at a yearly time scale (Jiang *et al.*, 2012; Zhu *et al.*, 2017). According to existing theories on the mechanism behind runoff-tide interactions, the residual water surface slope plays a pivotal role in the transformation between erosion and deposition in estuaries (Lamb *et al.*, 2012; Nittrouer *et al.*, 2012; Chatanantavet and Lamb, 2014; Cai *et al.*, 2014a, 2014b, 2016, 2018). A steep slope in residual water level forms when the river water discharge is high (Figure 3), which induces high seaward velocities that promote large fluxes of bed materials into the sea, causing erosion in estuarine areas. Conversely, a flat slope in residual water level appears at low river water discharge (Figure 3), which triggers small seaward velocities and relatively strengthens the backwater effect of the flood tide, facilitating sediment settling, landward transport of marine sediment, and hence the production of depositional features.

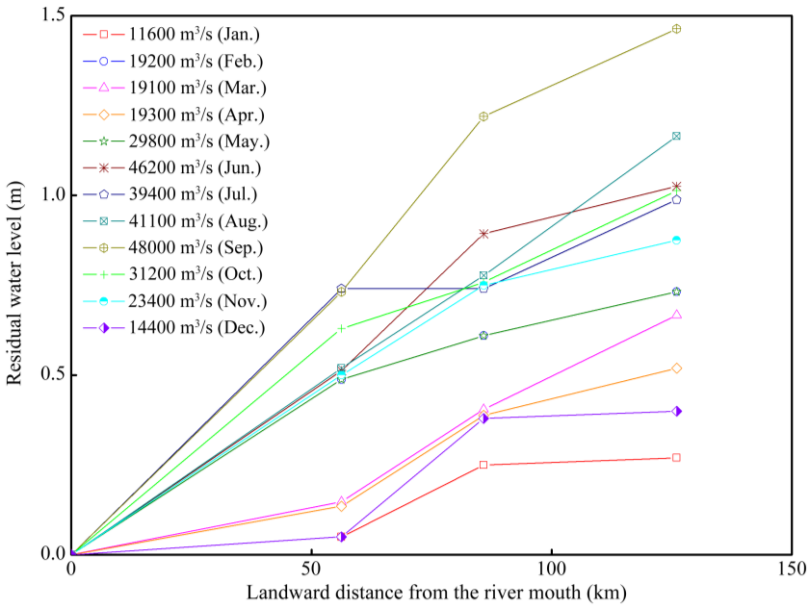

Figure 3 Residual water level with distance upstream from the Yangtze River mouth for varying monthly river water discharge in 2005.

Zhang's well-established formula for sediment transport capacity (Tan *et al.,* 2018) has previously been used, after modification to include marine influences in estuarine areas (see e.g. Xie and Yan, 2011; Mo *et al.*, 2012; Hu *et al.*, 2018). Given that we are mainly interested in the sediment transport capacity of the

Yangtze river water discharge, we employ the original version of Zhang's formula to determine the sediment transport capacity from:

$$S_* = k\left(\frac{U^3}{gR\omega}\right)^m \tag{8}$$

where k (kg/m^3) and m (-) are parameters with positive values calibrated using observed data; g (m/s^2) is the acceleration due to gravity; ω (m/s) is the settling velocity of sediment; U (m/s) is the depth-averaged river water flow velocity; and R (m) is the hydraulic radius. Using Manning's formula (see e.g. Hergarten and Neugebauer, 1997; Huang, 2007; Bao *et al.*, 2011):

$$U = \frac{1}{n} R^{2/3} J^{1/2} \tag{9}$$

Equation (8) can be rewritten as:

$$S_* = k\left(\frac{RJ^{\frac{3}{2}}}{gn^3\omega}\right)^m \tag{10}$$

where n (-) is Manning's roughness coefficient for the river bed, and J (-) is the water surface slope. Given that R in Equation (10) can be approximated by the water depth (h in m) for natural rivers where the channel width is much larger than water depth (Chai *et al.*, 2004), Equation (10) may also be expressed as:

$$S_* = k\left(\frac{hJ^{\frac{3}{2}}}{gn^3\omega}\right)^m \tag{11}$$

The parameters k, m, and n are calibrated from observed data, and are usually assigned constant values at fixed locations; and ω is closely related to the physico-chemical characteristics of sediment (Tan *et al.*, 2018). Therefore, S_* is mainly determined by $hJ^{\frac{3}{2}}$. As Figure 3 shows, high river water discharge occurs for large h and J, therefore resulting in S_* having a high value implying large sediment transport flux to the sea. Conversely, low river water discharge corresponds to low sediment flux entering the sea. Consequently, the alternate erosion and deposition in the Yangtze Estuary can be interpreted by the mechanism of interaction between runoff and flood tide. Since the peak values of monthly discharge of the three runoff flood periods (before 1958, 1997-2002 and 2009-2013) reached 84,200 m^3/s, 77,100 m^3/s, and 61,400 m^3/s

respectively, it can be speculated from Figure 3 and Equation (11) that the slopes in residual water level, water depth, and S_* should be very large during these periods; consequently, erosion has been generated in the entire estuary. In contrast, the following dry periods corresponded to low slopes in residual water level, water depth, and S_*, with obvious backwater effects and deposition resulting.

4.2.3 Impacts of other factors

Other than river fluxes and tidal currents, the Yangtze Estuary may also be affected by coastal dynamics (primarily from waves, sea level rise, and typhoons) and major estuarine engineering projects (Xuliujing Node narrowing, Deepwater Channel Project, and land reclamation).

Coastal dynamics.

According to existing studies (Wang *et al.*, 2008, 2013), the influence of waves and sea level change decays rapidly on reaching the mouth of the Yangtze Estuary, and therefore exerts very limited impact on its hydrodynamic-morphological changes. Therefore, the focus of the present discussion is on the impact of typhoons. In the East China Sea, typhoons act as a random forcing factor, which triggers storm surges and causes severe erosional or depositional changes in estuaries (Dai *et al.*, 2014a; Du *et al.*, 2019). Comparing the magnitudes (classes and increased water levels) of typhoons in the Yangtze estuarine area over the past 65 years (Table 3) with the erosional/depositional rates of the entire Yangtze Estuary during corresponding historical periods (Figure 2a), it can be judged that typhoons do not act as a controlling factor of morphological alternation. In detail, the average magnitudes of typhoons before 1983, during 1983-1997, and during 1997-2002 exhibit little difference, whereas the erosional/depositional rates of the entire Yangtze Estuary varied conspicuously. Similar behavior also occurs between the 2009-2013 and 2013-2015 periods (Table 3 and Figure 2a). Nonetheless, consecutive typhoon events in short time might incur remarkable changes to morphology, an example being the series of typhoons in 2015 that strengthened the flood-tide-driven sediment transport scoured from the offshore deep-water zone, and promoted heavy deposition in the Yangtze Estuary during 2013-2015 (Figure 2a) (Chen Y *et al.,* 2018).

Table 3 Major typhoons in the Yangtze estuarine area over the past 65 years.

Name	Time ((Day. Month. Year)	Max. wind power (class)	Increased water level at Wusong (m)
8114	1.9.1981	11-12	1.51
8310	27.9.1983	8-10	1.17
8615	27.8.1986	10	1.12
8913	4.8.1989	10	1.11
9711	18.8.1997	8-10	1.45
Prapiroon	31.8.2000	12	1.38
Saosmei	14.9.2000	8	1.29
Sinlaku	8.9.2002	7	0.96
Milei	25-26.6.2011	10	
Meihua	6-8.8.2011	13	
Sula	2.8.2012	12	
Dawei	2.8.2012	12	
Haikui	5-8.8.2012	15	
Bulawan	27-28.8.2012	15	
Tiancheng	29-30.8.2012	12	
Sanba	16-17.9.2012	16	
Feite	6-8.10.2013	14	
Dannasi	6-8.10.2013	14	
Huanxiong	7-10.7.2014	13	
Najili	1-3.8.2014	10	
Bapeng	4-6.10.2014	14	
Huangfeng	12.10.2014	11	
Series of typhoons	2015		

Estuarine engineering projects.

Since the 1960s, the upstream node of the Yangtze Estuary, the Xuliujing Node, has remained roughly stable, as its width was artificially narrowed to about 5.7 km (Yun, 2004; Wang *et al*., 2013). This has not produced notable impacts on river fluxes and morphological evolution in the Yangtze Estuary over the periods concerned in this study. In 1998, the Deepwater Channel Project was implemented in the North Passage (Figure 1b). Although this project has been associated with serious back-siltation in its vicinity, primarily in the North Passage (Luan *et al.*, 2016; Li *et al.*, 2018; Zhao *et al.*, 2018), deposition only become obvious after 2004, and has experienced upward and downward courses respectively before and after 2010, as reflected by the variation in yearly dredging quantity during 2000-2015 (Figure 4a). Back siltation induced by the channel project has not kept pace with the erosion-deposition alternation of the entire Yangtze Estuary (Figure 2a) and is unlikely to be a dominant factor. More precisely, the project-induced

multi-year average depositional rate in the North Passage during 2009-2013 was much larger than during 2002-2009 and 2013-2015 (Figure 4a), whereas the entire Yangtze Estuary underwent severe erosion during 2009-2013 and experienced deposition during the other two periods (Figure 4a). Land reclamation was mainly implemented on the tidal flats and along the North Branch (Figure 1b) (Dai *et al.*, 2016; Chen L *et al.*, 2018; Su and Fan, 2018; Teng *et al.*, 2019). Total reclamation in these areas during different periods (Figure 4b) has contributed significantly to deposition in the Yangtze Estuary in corresponding periods (Figure 2a). Nevertheless, reclamation has not determined the erosion-deposition alternation, because the reclamation rates during certain periods have not shown strong positive correlations with the erosional/depositional rates of the entire Yangtze Estuary during corresponding periods (Figure 4b). Hence, reclamation is not the determinant factor in the morphological alternation of the entire Yangtze Estuary.

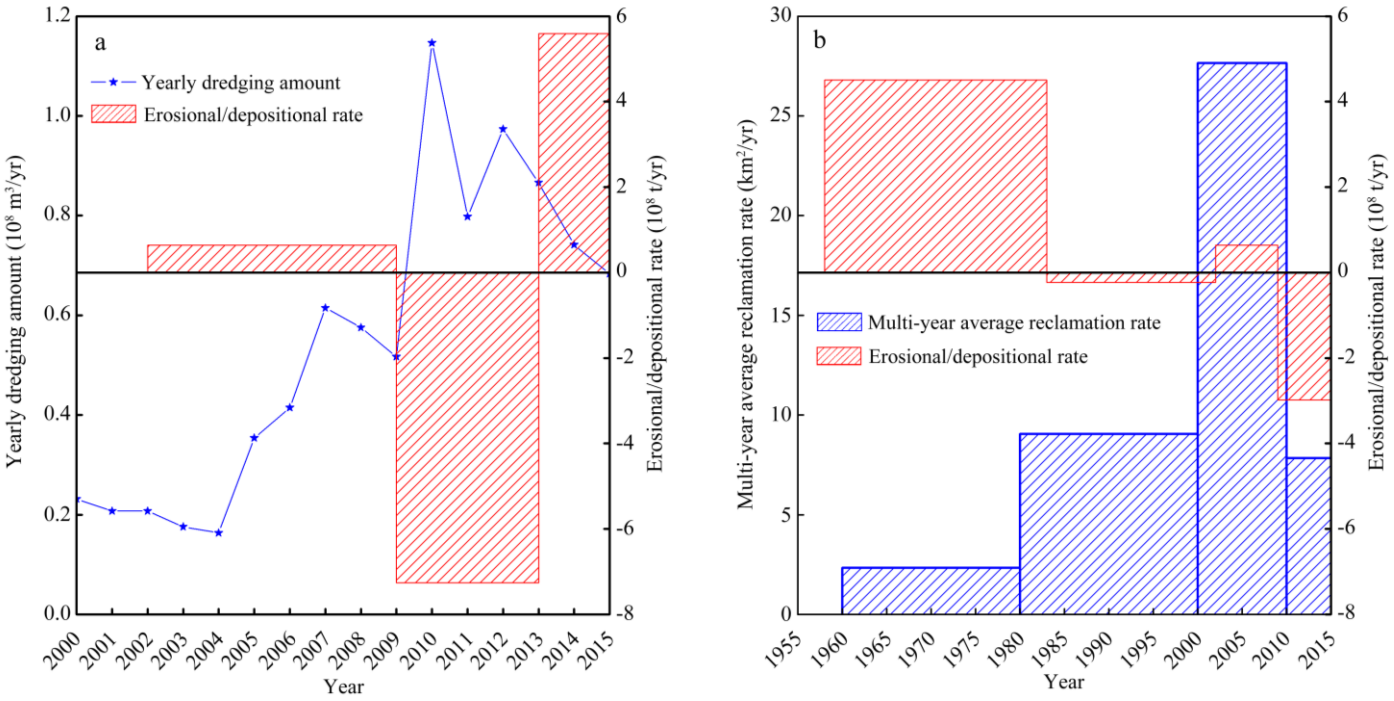

Figure 4 Yearly dredging volume of the Deepwater Channel Project from 2000 to 2015 (a) and multi-year average reclamation rates for the whole Yangtze Estuary during the periods of 1960-1980, 1980-2000, 2000-2010, and 2010-2015 (b) and erosional/depositional rates (positive values indicating deposition, and negative ones representing erosion) of the entire Yangtze Estuary during the corresponding periods ((a) and (b)).

In summary, neither the coastal dynamics nor the estuarine engineering projects play the dominant role in the erosion-deposition alternation of the entire Yangtze Estuary.

4.3 Post-TGD deposition

After the impoundment of the Three Gorges Dam (i.e. the post-TGD period), heavy deposition within the Yangtze Estuary has been reported by various researchers. For instance, Dai *et al.* (2014a) found that a high depositional rate of 229×10^6 m^3/yr occurred in the submerged delta (121.78° E - 122.67° E, 30.82° N - 31.53° N) of the Yangtze Estuary during the post-TGD period of 2002-2009, which was about twice as large as the rate of 118×10^6 m^3/yr during the pre-TGD period of 1958-2002. Chen Y *et al.* (2018) also indicated that high depositional rates during post-TGD periods of 2002-2009 and 2013-2015 have taken place in a large submerged area (containing the marked area in Figure 1b) from Xuliujing to the delta front in the Yangtze Estuary.

Within the framework interpreting the mechanism of the alternate pattern of erosion-deposition, such heavy deposition during the post-TGD period mainly resulted from the significant reduction in flood peaks after the impoundment of TGD (Zhu *et al.*, 2017; Fu, 2018; Mei *et al.*, 2018). As the occurrence frequency of low flow discharges increased, the residual water surface slope flattened, resulting in lower S_* and a more obvious backwater effect in the Yangtze Estuary, and hence considerable deposition. Figure 5 shows the distribution of bed-elevation change rates in the Yangtze mouth bar area (121.78° E - 122.34° E, 30.96° N - 31.46° N) during the post-TGD dry period of 2002-2007 in comparison with the pre-TGD flood period of 1997-2002. The overall bed-elevation depositional rate has increased significantly from the pre-TGD flood period to the post-TGD dry period, corresponding to a shift of $D_{\geq 60,000}$ (from 29 days/yr to 4 days/yr). Figure 5b shows that the Deepwater Channel Project has affected the local erosion-deposition pattern at the site, such as the obvious deposition along the two sides of the North Passage and the upper-reach erosion and lower-reach deposition in the South Passage, even though the channel project does not determine the overall morphological evolution of the Yangtze Estuary.

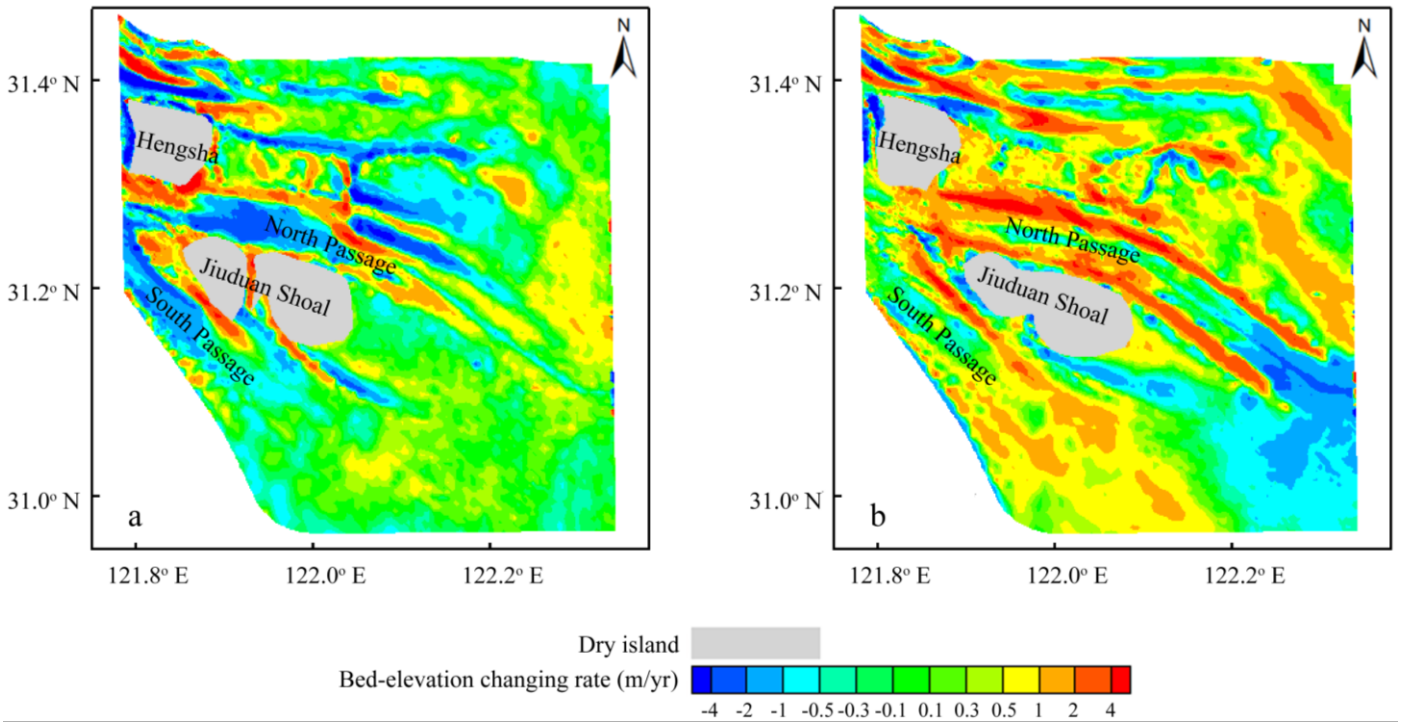

Figure 5 Spatial distribution of bed-elevation change rates (positive values indicating deposition, and negative ones representing erosion) in the Yangtze mouth bar area (121.78° E - 122.34° E, 30.96° N - 31.46° N) during the periods of (a) 1997-2002, and (b) 2002-2007.

Figure 6 illustrates the sediment budget of the Yangtze Estuary during the post-TGD period from 2002 to 2009. Even though we assume that all the sediment load from Xuliujing was deposited within the three areas marked by dashed lines in Figure 6, the load only contributes 48-64% of the deposition in these areas. If deposition from the seaward sediment flux (i.e., 0.46×10^8 t/yr implied in Figure 6) in the area between Xuliujing and the river mouth is taken into account, it appears that the contribution of marine source brought by the flood tide to the post-TGD heavy deposition was at least 36-52%. Similarly, sediment load from Xuliujing during 2013-2015 was extremely low, also implying a great contribution from the marine source to Area 3 (Figure 6c) where heavy deposition occurred in the corresponding period (Chen Y *et al.*, 2018). It should be noted that there was no directly observed data on sediment load at Xuliujing during 2013-2015. However, a positive relationship has been found between sediment load at Datong and that at Xuliujing (Yang Y P *et al.*, 2015), and so the low sediment supply from Xuliujing during 2013-2015 could be fairly represented by that from Datong (Figure 2b). Previous research (Liu *et al.*, 2011; Li *et al.*, 2019) has also

shown that sediment in the Yangtze Estuary comes from both river and sea, through analyses of the particle sizes of bed materials, and suggested that the available fine sediment supplied to the estuary from the offshore area is abundant, supporting the present findings.

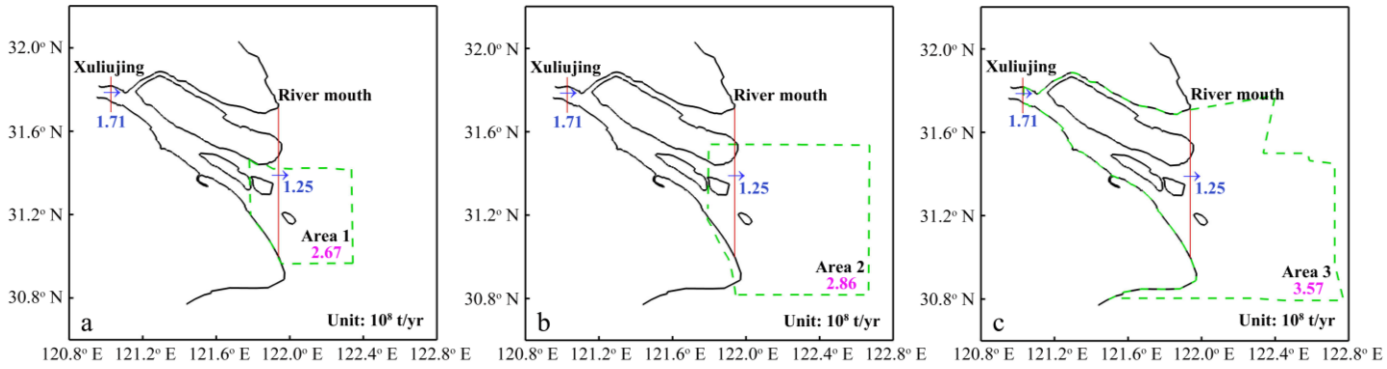

Figure 6 Comparison of net sediment supplies at Xuliujing and the Yangtze River mouth with depositional rates within (a) Area 1, (b) Area 2 and (c) Area 3 during 2002-2009. Specifically, Area 1 represents the mouth bar area (121.78° E - 122.34° E, 30.96° N - 31.46° N) in Figure 5, Area 2 the submerged delta (121.78° E - 122.67° E, 30.82° N - 31.53° N) considered by Dai *et al.* (2014a), and Area 3 the large submerged area of the entire Yangtze Estuary downstream of Xuliujing considered by Chen Y *et al.* (2018). In addition, the blue numbers represent net sediment fluxes at Xuliujing and the Yangtze River mouth, whereas the magenta numbers indicate depositional rates in the three areas.

4.4 Future morphological change

Since 1950, more than 50,000 dams have been constructed in the Yangtze River Basin (Yang *et al.*, 2011). Under the operation of these dams, the seasonal distribution of runoff discharge has been smoothed, mainly resulting in decreased multi-year average duration days for discharge levels < 10,000 m^3/s and > 50,000 m^3/s, and increased duration days for discharges in the range 10,000-20,000 m^3/s (Figure 7). In particular, $D_{\geqslant 60,000}$ decreased to 3 days/yr during the post-TGD period of 2003-2015. According to existing studies (Expert Group of Sediment Problem of the Office of the Three Gorges Project Construction Committee of the State Council, Expert Group of Sediment Problem of the Three Gorges Project of the China Changjiang Three Gorges Project Development Corporation, 2002; Yang S L *et al.*, 2007, 2014), the future multi-year average river sediment load entering into the Yangtze Estuary will not surpass 1.5×10^8 t/yr within 300 years. If this limitation of sediment load is adopted and the multi-year average runoff volume is

taken to be 8923×10^8 m^3/yr (average value of 1950-2015), the critical $D_{\geqslant 60,000}$ related to morphological equilibrium of the entire Yangtze Estuary is deduced as 14 days/yr using Equation (7), which is significantly larger than 3 days/yr during 2003-2015. At the time of writing, a cascade of large dams is under construction along the upper Yangtze, leading to continuous "smoothing" of the river water discharge due to the water regulation (Duan *et al.*, 2016). Therefore, it is not likely that the multi-year average $D_{\geqslant 60,000}$ will exceed 14 days/yr in the future. Consequently, the residual water surface slope will be further flattened, resulting in lower S_* and more significant backwater effects in the Yangtze Estuary. Hence, deposition may still occur in the Yangtze Estuary, especially if the sediment supply from the offshore area is abundant when discharge "smoothing" occurs.

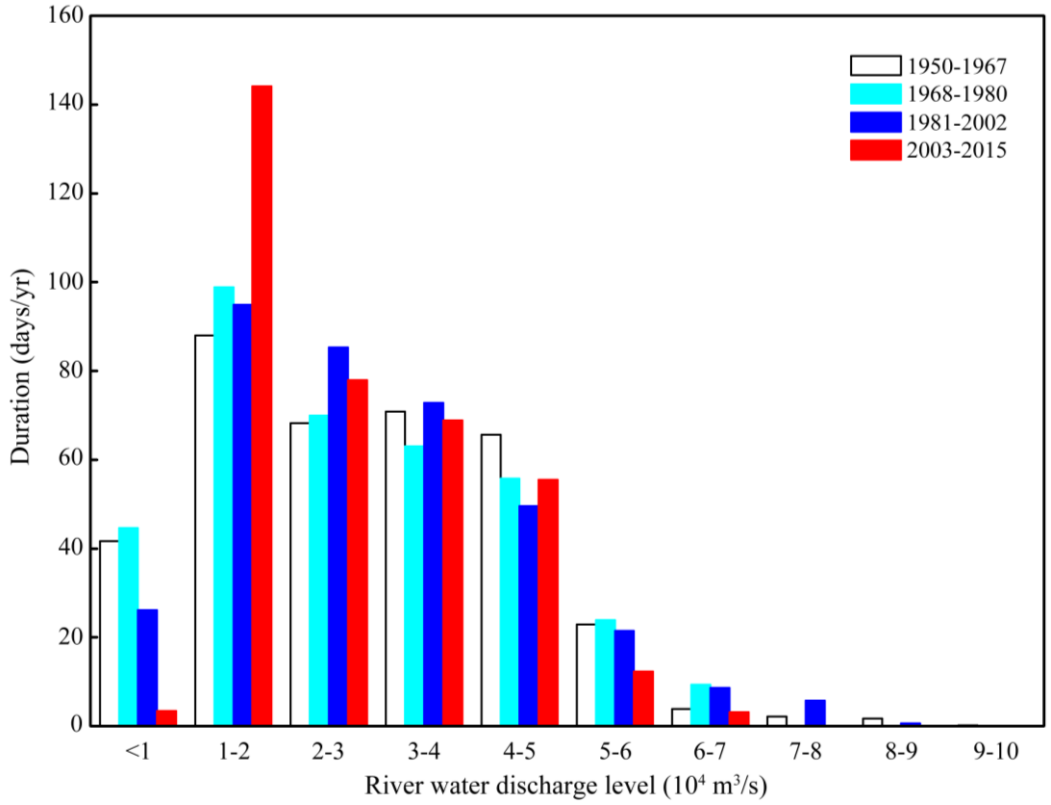

Figure 7 Histogram of multi-year average duration days at different levels of river water discharge at Datong during different stages of the construction of major dams on the Yangtze River. The dividing years of 1968, 1981 and 2003 correspond to the impoundments of Danjiangkou Dam, Gezhou Dam, and Three Gorges Dam (Figure 1a).

Nonetheless, the mean depositional rate of the entire Yangtze Estuary greatly depends on changes in total sediment flux from the Yangtze River Basin, the Yellow River Delta, and Hangzhou Bay. In the past 50

years, sediment supply from the Yangtze River has presented a declining trend due to the construction of dams and the implementation of soil conservation measures within the river basin (Yang *et al.*, 2011; Luo *et al.*, 2017; Yang *et al.*, 2018), as evidenced by the decreased suspended sediment concentrations at Datong and Xuliujing (Figure 8a). Similarly, sediment supply from the Yellow River Delta has also experienced a decreasing trend because of dam-based water-sediment regulation schemes in the basin, which have reduced the river-to-sea sediment load of the Yellow River (Chu, 2014; Tan *et al.*, 2016). Such reduction can be discerned by the decreases in suspended sediment concentration of the Yellow River mouth and the Laizhou Bay since 2003 (Figure 8b). Sediment supply from the Hangzhou Bay also reduced, as evident by the decreases in suspended sediment concentration at the gauge stations in the bay after 2002 (Figure 8c), mainly due to the construction of dams and sluices on the rivers discharging sediment into the bay (Zeng, 2010; Li, 2012; Dai *et al.*, 2014b). The decreasing trends in sediment flux from all three sources imply that the mean depositional rate of the entire Yangtze Estuary is not likely to exceed the peak value of the past fifty years.

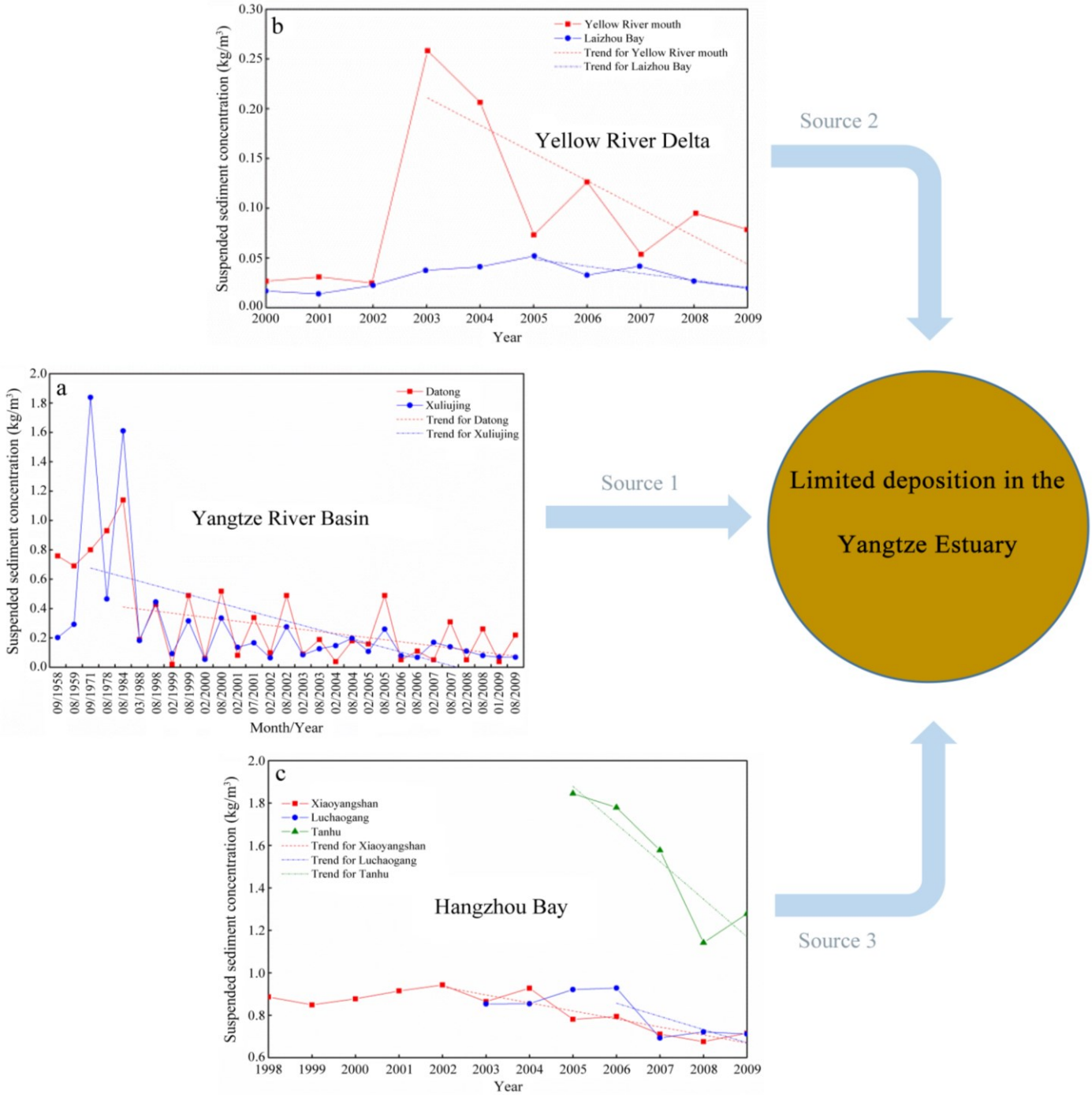

Figure 8 Temporal variations in suspended sediment concentration in (a) the Yangtze River Basin, (b) the Yellow River Delta and (c) Hangzhou Bay, and the consequent morphological change rate for the entire Yangtze Estuary in the future.

5 Conclusions

Alternations between erosion and deposition have occurred in the entire Yangtze Estuary under the hydrological cycles between flood and dry periods in the river basin over the past 65 years. Erosion came with flood events and deposition followed with dry flows. The study demonstrated that the erosional/depositional rate of the entire Yangtze Estuary related quantitatively to the annual river water

discharge, $D_{\geq 60,000}$ and yearly river sediment load, with contributing proportions of 1%, 59% and 40%, respectively. The morphology-hydrology process was further interpreted using the residual water surface slope and the corresponding sediment transport capacity. It was found that coastal dynamics and estuarine engineering projects altered local morphological changes, but hardly affected the total erosional/depositional rate of the whole estuarine region. Post-TGD heavy deposition within the Yangtze Estuary can be attributed to the truncation of flood peaks due to water regulation by TGD, with much of the sediment (between 36 and 52%) supplied at flood tide from the sea. A critical value of $D_{\geq 60,000}$ corresponding to the future equilibrium state of the Yangtze Estuary is estimated at about 14 days/yr. However, the future multi-year average $D_{\geq 60,000}$ is unlikely to exceed this value because the river water discharge will be continuously smoothed by the cascade of large dams along the upper Yangtze. Therefore, deposition may still occur in the Yangtze Estuary. However, the mean depositional rate is not likely to exceed the peak value of the past, because the sediment loads from the three sources, i.e., the Yangtze River Basin, the Yellow River Delta and the Hangzhou Bay have all presented decreasing trends. The findings of this study have implications for other estuaries worldwide that are experiencing substantial hydrological, sediment, climate, and anthropogenic changes.

References

Andrews E D, 1980. Effective and bankfull discharges of streams in the Yampa River Basin, Colorado and Wyoming. *Journal of Hydrology*, 46(3-4): 311-330.

Bao W M, Zhang X Q, Yu Z B *et al*., 2011. Real-time equivalent conversion correction on river stage forecasting with Manning's Formula. *Journal of Hydrological Engineering*, 16(1): 1-9.

Cai H Y, Savenije H H G, Jiang C J, 2014a. Analytical approach for predicting fresh water discharge in an estuary based on tidal water level observations. *Hydrology and Earth System Sciences*, 18(10): 4153-4168.

Cai H Y, Savenije H H G, Toffolon M, 2014b. Linking the river to the estuary: influence of river discharge on tidal damping. *Hydrology and Earth System Sciences*, 18(1): 287-304.

Cai H Y, Savenije H H G, Jiang C J et al., 2016. Analytical approach for determining the mean water level profile in an estuary with substantial fresh water discharge. *Hydrology and Earth System Sciences*, 20(3): 1177-1195.

Cai H Y, Yang Q S, Zhang Z H *et al*., 2018. Impact of river-tide dynamics on the temporal-spatial distribution of residual water level in the Pearl River channel networks. *Estuaries & Coasts*, 2018(10):1-19.

Chai J C, Miura N, Nomura T, 2004. Effect of hydraulic radius on long-term drainage capacity of geosynthetics drains. *Geotextiles Geomembranes*, 22(1-2): 3-16.

Changjiang Water Resources Commission (CWRC), 2015. *Changjiang River Sediment Bulletin*. Changjiang Press: Wuhan, China. (in Chinese)

Chatanantavet P, Lamb M P, 2014. Sediment transport and topographic evolution of a coupled river and river plume system: An experimental and numerical study. *Journal of Geophysical Research - Earth Surface*, 119(6): 1263-1282.

Chen J, Li D, 2002. *Regulation of the Changjiang Estuary: Past, Present and Future*. Springer Netherlands: Berlin, Germany, 185-197 pp.

Chen J Y, Yun C X, Xu H, 1982. *The Model of Development of the Changjiang Estuary During the Last 2000 years*. Academic Press: New York, America, 655-666 pp.

Chen L, Ren C Y, Zhang B *et al*., 2018. Spatiotemporal dynamics of coastal wetlands and reclamation in the Yangtze Estuary during past 50 years (1960s-2015). *Chinese Geographical Science*, 28(3): 386-399.

Chen Y, Dong J W, Xiao X M *et al*., 2016. Land claim and loss of tidal flats in the Yangtze Estuary. *Scientific Reports*, 6: 24018.

Chen Y, Wang H M, Shi Y J *et al*., 2018. Characteristics and trends of morphological evolution of the Yangtze subaqueous delta during 1958-2015. *Advances in Water Science*, 29(3): 314-321. (in Chinese)

Chu Z X, 2014. The dramatic changes and anthropogenic causes of erosion and deposition in the lower Yellow (Huanghe) River since 1952. *Geomorphology*, 216: 171–179.

Cooper J A G., 2002. The role of extreme floods in estuary-coastal behaviour: contrasts between river- and tide-dominated microtidal estuaries. *Sedimentary Geology*, 150(1-2): 123-137.

Dai Z J, Fagherazzi S, Mei X F *et al*., 2016. Linking the infilling of the North Branch in the Changjiang (Yangtze) estuary to anthropogenic activities from 1958 to 2013. *Marine Geology*, 379: 1-12.

Dai Z J, Liu J T, Fu G *et al*., 2013. A thirteen-year record of bathymetric changes in the North Passage, Changjiang (Yangtze) estuary. *Geomorphology*, 187: 101-107.

Dai Z J, Liu J T, Wei W, 2015. Morphological evolution of the South Passage in the Changjiang (Yangtze River) estuary, China. *Quaternary International*, 380: 314-326.

Dai Z J, Liu J T, Wei W *et al*., 2014a. Detection of the Three Gorges Dam influence on the Changjiang (Yangtze River) submerged delta. *Scientific Reports*, 4: 6600.

Dai Z J, Liu J T, Xie H L *et al.*, 2014b. Sedimentation in the outer Hangzhou Bay, China: The influence of Changjiang sediment load. *Journal of Coastal Research*, 30(6): 1218-1225.

Du J B, Park K, Dellapenna T M *et al.*, 2019. Dramatic hydrodynamic and sedimentary responses in Galveston Bay and adjacent inner shelf to Hurricane Harvey. *Science of the Total Environment*, 653: 554-564.

Du J L, Yang S L, Feng H, 2016. Recent human impacts on the morphological evolution of the Yangtze River delta foreland: A review and new perspectives. *Estuarine, Coastal and Shelf Science*, 181: 160-169.

Duan W X, Guo S L, Wang J *et al*., 2016. Impact of cascaded reservoirs group on flow regime in the middle and lower reaches of the Yangtze River. *Water*, 8(6): 1-21.

Emmett W W, Wolman M G, 2001. Effective discharge and gravel-bed rivers. *Earth Surface Processes Landforms*, 26(13): 1369-1380.

Expert Group of Sediment Problem of the Office of the Three Gorges Project Construction Committee of the State Council, Expert Group of Sediment Problem of the Three Gorges Project of the China Changjiang Three Gorges Project Development Corporation, 2002. Research on the sediment problem of the Changjiang Three Gorges Project (1996-2000)—the synthetic analysis of the 1995s' sediment research of the Changjiang Three Gorges Project. Beijing: Intellectual Property Publishing House Co., Ltd., 8: 5-100. (in Chinese)

Fu G, 2018. Recent changes of runoff, sediment discharge and suspended sediment particle size in the Yangtze estuary. *Port*

& Waterway Engineering, (2): 105-110. (in Chinese)

Gomez B, Coleman S E, Sy V W K et al., 2007. Channel change, bankfull and effective discharges on a vertically accreting, meandering, gravel-bed river. *Earth Surface Processes and Landforms*, 32(5): 770-785.

Guo L C, van der Wegen M, Roelvink D *et al*., 2015. Exploration of the impact of seasonal river discharge variations on long-term estuarine morphodynamic behavior. *Coastal Engineering*, 95: 105-116.

He Y F, Chen H Q, Chen J Y, 2013. Morphological evolution of mouth bars on the Yangtze estuarine waterways in the last 100 years. *Journal of Geographical Sciences*, 23(2): 219-230.

Hergarten S, Neugebauer H J, 1997. Homogenization of Manning's formula for modeling surface runoff. *Geophysical Research Letters*, 24(8): 877-880.

Hu X Z, Yang F, Song L X et al., 2018. An unstructured-grid based morphodynamic model for sandbar simulation in the Modaomen Estuary, China. *Water*, 10(5): 611.

Huang S L, 2007. Effects of using different sediment transport formulae and methods of computing Manning's roughness coefficient on numerical modeling of sediment transport. *Journal of Hydraulic Research*, 45(3): 347-356.

Jiang C J, Li J F, de Swart H E, 2012. Effects of navigational works on morphological changes in the bar area of the Yangtze Estuary. *Geomorphology*, 139: 205-219.

Lamb M P, Nittrouer J A, Mohrig D *et al*., 2012. Backwater and river plume controls on scour upstream of river mouths: Implications for fluvio-deltaic morphodynamics. *Journal of Geophysical Research - Earth Surface*, 117: F01002.

Li L X, Pan Y, Li L, 2018. Fractal characteristics and prediction of backsilting quantity in Yangtze Estuary Deepwater Channel. *China Ocean Engineering*, 32(3): 341-346.

Li M T, Chen Z Y, Yin D W *et al*., 2011. Morphodynamic characteristics of the dextral diversion of the Yangtze River mouth, China: tidal and the Coriolis Force controls. *Earth Surface Processes and Landforms*, 36(5): 641-650.

Li P, 2012. Variations in Estuarine and Coastal Suspended Sediment Concentration and Delta Accretion/Erosion in Response to Decline in Sediment Supply From the Yangtze River, PhD Thesis. State Key Laboratory of Estuarine and Coastal Research, East China Normal University, Shanghai, China. (in Chinese)

Li X, Liu J P, Tian B, 2016. Evolution of the Jiuduansha wetland and the impact of navigation works in the Yangtze Estuary, China. *Geomorphology*, 253: 328-339.

Li Y M, Zhang G A, You B W *et al.*, 2019. Recent sediment characteristics and their impact factors in the Yangtze Estuary riverbed. *Acta Geographica Sinica*, 74(1): 178-190. (in Chinese)

Lin C K, 1988. Quantity and transport of sediment at the Yangtze River Estuary. *Scientia Sinica Series A-Mathematical Physical Astronomical & Technical Sciences*, 31(12): 1495-1507.

Liu H, He Q, Gert J W *et al.*, 2011. Sediment exchange and transport processes in the Yangtze River Estuary: Concurrent discussion on the effects of sediment sink in the muddy area. *Acta Geographica Sinica*, 66(3): 291-304. (in Chinese)

Liu J, Cheng H F, Han L *et al.*, 2019. Interannual variations on siltation of the 12.5 m deepwater navigation channel in Yangtze Estuary. *Advances in Water Sciences*, 30(1): 65-75. (in Chinese)

Luan H L, Ding P X, Wang Z B *et al*., 2017. Process-based morphodynamic modeling of the Yangtze Estuary at a decadal timescale: Controls on estuarine evolution and future trends. *Geomorphology*, 290: 347-364.

Luan H L, Ding P X, Wang Z B *et al*., 2016. Decadal morphological evolution of the Yangtze Estuary in response to river input changes and estuarine engineering projects. *Geomorphology*, 265: 12-23.

Luo X X, Yang S L, Wang R S *et al*., 2017. New evidence of Yangtze delta recession after closing of the Three Gorges Dam. *Scientific Reports*, 7: 41735.

Mei X F, Dai Z J, Wei W *et al*., 2018. Secular bathymetric variations of the North Channel in the Changjiang (Yangtze) Estuary, China, 1880-2013: Causes and effects. *Geomorphology*, 303: 30-40.

Mo W Y, Wei X, Qiu L G, 2012. A long-term numerical model of morphodynamic evolution and its application to the Modaomen Estuary. *China Ocean Engineering*, 26(1):123-138.

Nittrouer J A, Shaw J, Lamb M P *et al*., 2012. Spatial and temporal trends for water-flow velocity and bed-material sediment transport in the lower Mississippi River. *Geological Society of America Bulletin*, 124(3-4): 400-414.

Su J F, Fan D D, 2018. Internal facies architecture and evolution history of Changxing mouth-bar complex in the Changjiang (Yangtze) Delta, China. *Journal of Ocean University of China*, 17(6): 1281-1289.

Tan C, Huang B S, Liu F *et al*., 2016. Transformation of the three largest Chinese river deltas in response to the reduction of sediment discharges. *Journal of Coastal Research*, 32(6): 1402-1416.

Tan G M, Fang H W, Dey S *et al*., 2018. Rui-Jin Zhang's Research on Sediment Transport. *Journal of Hydraulic Engineering*, 144(6): 02518002.

Teng L Z, Cheng H Q, Qiao Y Y, 2019. Analysis of flow regime in the Turbidity Maximum Zone of Yangtze Estuary based on texture features of Tiangong-2 remote sensing images. In: Gu Y, Gao M, Zhao G (eds) Proceedings of the Tiangong-2 Remote Sensing Application Conference. *Lecture Notes in Electrical Engineering*, vol 541. Springer, Singapore.

Wang Y H, Dong P, Oguchi T *et al*., 2013. Long-term (1842-2006) morphological change and equilibrium state of the Changjiang (Yangtze) Estuary, China. *Continental Shelf Research*, 56: 71-81.

Wang Y H, Ridd P V, Wu H L *et al*., 2008. Long-term morphodynamic evolution and the equilibrium mechanism of a flood channel in the Yangtze Estuary (China). *Geomorphology*, 99(1-4): 130-138.

Wei W, Dai Z J, Mei X F *et al.*, 2017. Shoal morphodynamics of the Changjiang (Yangtze) estuary: Influences from river damming, estuarine hydraulic engineering and reclamation projects. *Marine Geology*, 386: 32-43.

Wei W, Mei X F, Dai Z J *et al*., 2016. Recent morphodynamic evolution of the largest uninhibited island in the Yangtze (Changjiang) estuary during 1998-2014: Influence of the anthropogenic interference. *Continental Shelf Research*, 124: 83-94.

Wu H L, Shen H T, Wang Y H, 2003. Evolution of mouth bars in the Changjiang Estuary, China: A GIS supporting study, *Paper Presented at International Conference on Estuaries and Coasts*, Hangzhou, China: 205-213.

Xia J Q, Li X J, Zhang X L *et al*., 2014. Recent variation in reach-scale bankfull discharge in the Lower Yellow River. *Earth Surface Processes and Landforms*, 39(6): 723-734.

Xie J, Yan Y X, 2011. Promoting siltation effects and impacts of Hengsha East Shoal on the Yangtze River estuary. *Journal of Hydrodynamics*, 23(5): 649-659.

Yang H F, Yang S L, Meng Y *et al*., 2018. Recent coarsening of sediments on the southern Yangtze subaqueous delta front:

A response to river damming. *Continental Shelf Research*, 155: 45-51.

Yang S L, Milliman J D, Li P *et al*., 2011. 50,000 dams later: Erosion of the Yangtze River and its delta. *Global and Planetary Change*, 75(1-2): 14-20.

Yang S L, Milliman J D, Xu K H *et al.*, 2014. Downstream sedimentary and geomorphic impacts of the Three Gorges Dam on the Yangtze River. *Earth-Science Reviews*, 138: 469-486.

Yang S L, Xu K H, Milliman J D *et al*., 2015. Decline of Yangtze River water and sediment discharge: Impact from natural and anthropogenic changes. *Scientific Reports*, 5: 12581.

Yang S L, Zhang J, Xu X J, 2007. Influence of the Three Gorges Dam on downstream delivery of sediment and its environmental implications, Yangtze River. *Geophysical Research Letters*, 34(10): L10401.

Yang Y P, Deng J Y, Zhang M J *et al*., 2015. The synchronicity and difference in the change of suspended sediment concentration in the Yangtze River Estuary. *Journal of Geographical Sciences*, 25(4): 399-416.

Yang Y P, Li Y T, Sun Z H *et al*., 2014. Suspended sediment load in the turbidity maximum zone at the Yangtze River Estuary: The trends and causes. *Journal of Geographical Sciences*, 24(1): 129-142.

Yun C X, 2004. *Recent Developments of the Changjiang Estuary*. China Ocean Press: Beijing, China, 31-47, 108-114 pp. (in Chinese)

Zeng J, 2010. Data Mining – Based Characteristics of Flow and Sediment Transport in Qiantang Estuary, PhD Thesis. College of Civil Engineering and Architecture, Zhejiang University, Hangzhou, China. (in Chinese)

Zhang M, Townend I, Zhou Y X *et al*., 2016. Seasonal variation of river and tide energy in the Yangtze estuary, China. *Earth Surface Processes and Landforms*, 41(1): 98-116.

Zhang M W, Dong Q, Cui T W *et al*., 2014. Suspended sediment monitoring and assessment for Yellow River estuary from Landsat TM and ETM plus imagery. *Remote Sensing of Environment*, 146(SI): 136-147.

Zhang Y F, Zhang Z K, Ren H *et al*., 2018. The sedimentation rates of tidal flat and environmental significance at Qidong foreland of the Yangtze Estuary. *Transactions of Oceanology and Limnology*, (4): 36-43. (in Chinese)

Zhao J, Guo L C, He Q *et al.*, 2018. An analysis on half century morphological changes in the Changjiang Estuary: Spatial

variability under natural processes and human intervention. *Journal of Marine Systems*, 181: 25-36.

Zheng S W, Cheng H Q, Shi S Y *et al.*, 2018. Impact of anthropogenic drivers on subaqueous topographical change in the Datong to Xuliujing reach of the Yangtze River. *Science China-Earth Sciences*, 61(7): 940-950.

Zhu B Y, Li Y T, Yue Y *et al*., 2017. Aggravation of north channels' shrinkage and south channels' development in the Yangtze Estuary under dam-induced runoff discharge flattening. *Estuarine Coastal and Shelf Science*, 187: 178-192.

Zhu L, He Q, Shen J *et al.*, 2016. The influence of human activities on morphodynamics and alteration of sediment source and sink in the Changjiang Estuary. *Geomorphology*, 273: 52-62.